3. Site specific recombination system *Streptococcus pyogenes* β recombinase

3.1. Results

3.1.1. Circular dichroism spectropolarimetry

The far-UV circular dichroism spectra of the 205 amino acid β recombinase in 50 mM sodium phosphate buffer pH 7.5, 1 M NaCl, and 5% glycerol (buffer I) measured at 25 °C revealed minima at 209 and 222 nm (Figure 3.1). About 48% α-helix, 13% β-sheet and 15% β-turn structures were calculated with the Variable Selection Method (VARSLC1). The calculated VARSLC1 results are in reasonable agreement with the content of 48% α-helices, 10% β-strands and 36 % turns predicted from the amino acid sequence of β recombinase with the "Network Protein Sequence Analysis server" and with the structure of the ordered γδ resolvase bound to site I (*46*).

3.1.2. Examination of β recombinase unfolding by intrinsic tyrosine fluorescence

The fluorescence emission spectrum of β recombinase in buffer I had the maximum near 305 nm as expected for selectively excited tyrosine residues (Figure 3.2). In β-Rec monomer, six tyrosine residues and no tryptophan are present. Unfortunately, the native tyrosine residues in the primary structure of β recombinase were not useful as a structural probe. Increasing urea concentrations from 0 to 6 M resulted in a gradual increase in fluorescence intensity only suggesting increasing number of exposed tyrosine residues. Moreover, fluorescence spectra showed that the samples were not contaminated by tryptophan containing impurities.

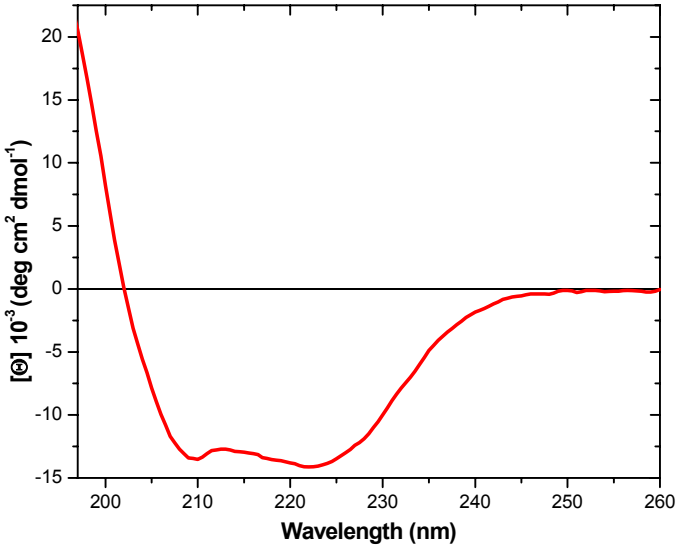

Figure 3.1: Far-UV CD Spectra of β recombinase. CD was measured at 25°C at a concentration of 16 µM β_2 in buffer I (50 mM sodium phosphate buffer, 1 M NaCl and 5% glycerol, pH 7.5).

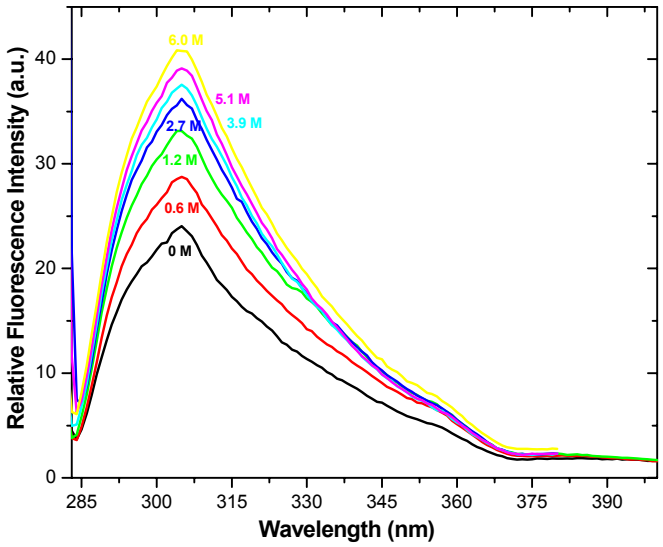

Figure 3.2: Fluorescence emission spectra at varying urea concentrations as indicated in the Figure. Protein concentration was 1.8 µM β_2 in buffer I (50 mM sodium phosphate buffer,1 M NaCl and 5% glycerol, pH 7.5); measurements at 25°C.

3.1.3. Hydrodynamic properties and stoichiometry

Gel filtration experiments revealed β recombinase dimers (β_2) in buffer I (Figure 3.3). Its dimeric state did not change up to 2 M sodium chloride in buffer I within the temperature range of 4 °C and room temperature. At concentrations of 16 µM to 42 µM β_2, symmetrical single elution peaks were observed with apparent molecular masses in the range of 52±2 kDa. The observed molar masses exceeded the theoretical mass of ~47.6 kDa β_2; this might either indicate the presence of higher oligomeric forms or effects of a non-globular shape of the molecules.

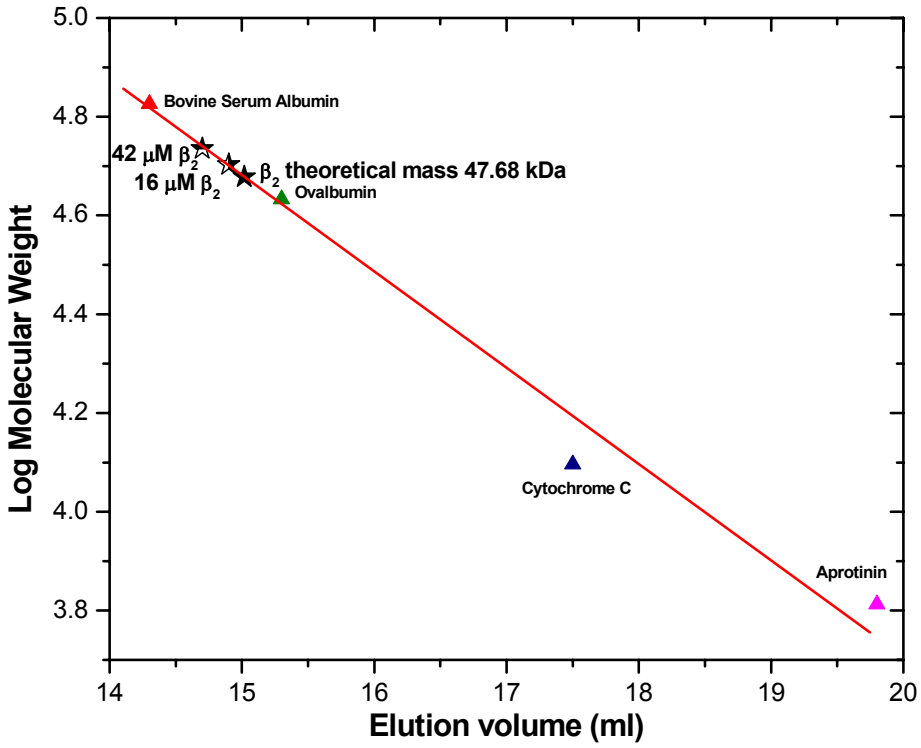

Figure 3.3: Size exclusion chromatography of β recombinase. Molecular standards for calibration curve were: Bovine serum albumin (67 kDa); Ovalbumin (43 kDa); Cytochrome C (12.5 kDa) and Aprotinin (6.5 kDa). The apparent molecular masses of β recombinase are ~50 kDa and ~54 kDa for an input concentration of 16 µM and 42 µM in dimer equivalents (β_2), respectively. The theoretical mass of β_2 is 47.7 kDa.

Results of analytical ultracentrifugation are shown in Figure 3.4. β recombinase had a molar mass of ~ 48 kDa in the concentration range 3 μM to 17 μM in buffer I that indicated the presence of stable β_2. However, a molar mass of ~80 to ~ 90 kDa was observed in buffer with 0.5 M NaCl that pointed to the formation of higher oligomeric forms (data not shown). Moreover, the β recombinase was also studied in the presence of urea. At 5 M urea with β monomer concentrations between 4 μM to 18 μM; molar masses of 23.5±1 kDa were observed, revealing a dissociation of dimer to monomers (Figure 3.4). Molecular masses of 23.5±1 kDa were found in 8 M urea at β monomer concentrations of 22 μM to 44 μM; in agreement with the expected presence of monomers under those conditions (Figure 3.4).

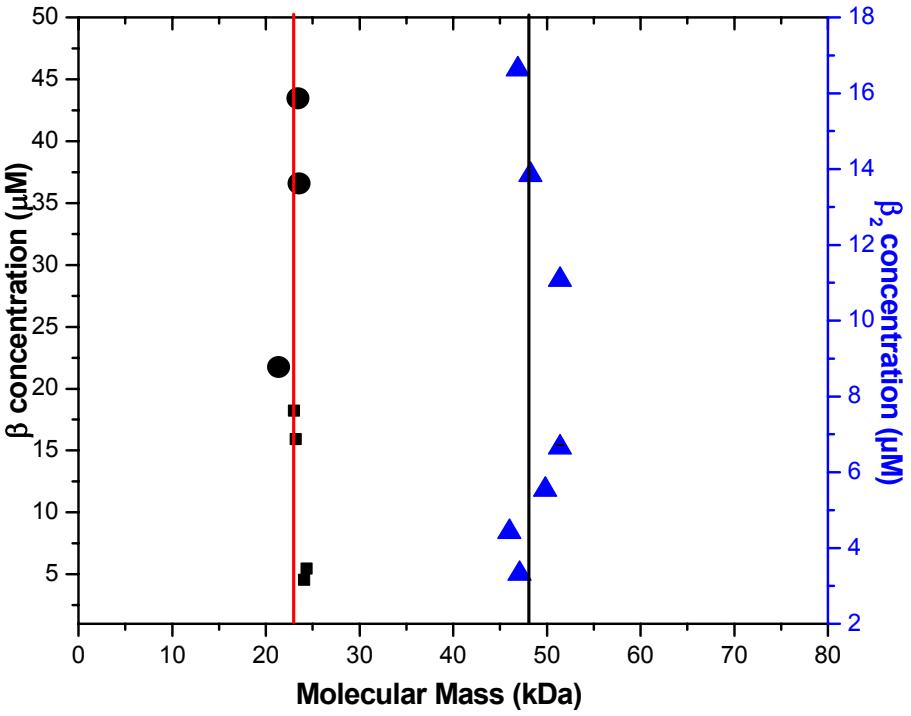

Figure 3.4: Analytical ultracentrifugation of β recombinase. The blue triangles, black squares and black circles corresponds to buffer I (50 mM sodium phosphate, 1 M NaCl and 5% glycerol, pH 7.5), buffer I + 5 M urea and buffer I + 8 M urea, respectively. Red and bleck lines correspond to molecular masses of β and β_2, respectively.

3.1.4. Denaturant-induced unfolding

Unfolding of β recombinase by urea and Gdn-HCl was monitored measuring changes of the CD at 222 nm (Figure 3.5). Denaturation curves of β_2 as function of either urea or Gdn-HCl were biphasic with a bend at 5 M urea and 2.2 M Gdn-HCl. The CD data scattered markedly at low denaturant concentrations that might have simply indicated dissolution of aggregated protein molecules and between 0 M and 2 M urea a more negative ellipticity was observed. Between 2 and 5 M urea the molar mean residue ellipticity decreased linearly from ~ $-14 \cdot 10^3$ deg cm^2/dmol to ~ $-9 \cdot 10^3$ deg cm^2/dmol followed by a section of the unfolding curve with steeper slope. Plateau values of about $-2 \cdot 10^3$ deg cm^2/dmol were reached at ~ 7 M urea. To further probe the unfolding of β recombinase, we conducted experiments that examined the protein concentration dependence of unfolding. Small change was observed in transition profiles obtained at β monomer concentrations of 3.65 and 36.5 μM (Figure 3.5).

Our denaturant induced unfolding results reveal that the monitored structural transitions can be described in terms of a three-state process in which β_2 unfolds from fully folded (N_2) state via an intermediate state (I) to unfolded state (U) according to model 3.1

$$N_2 \leftrightarrow 2I \leftrightarrow 2U \qquad \text{Model 3.1}$$

Fitting of the experimental unfolding curves as described in appendix [Section 9.1.2. (B) (I)] for the three-state model with monomeric intermediate results in thermodynamic parameters given in Table 3.1.

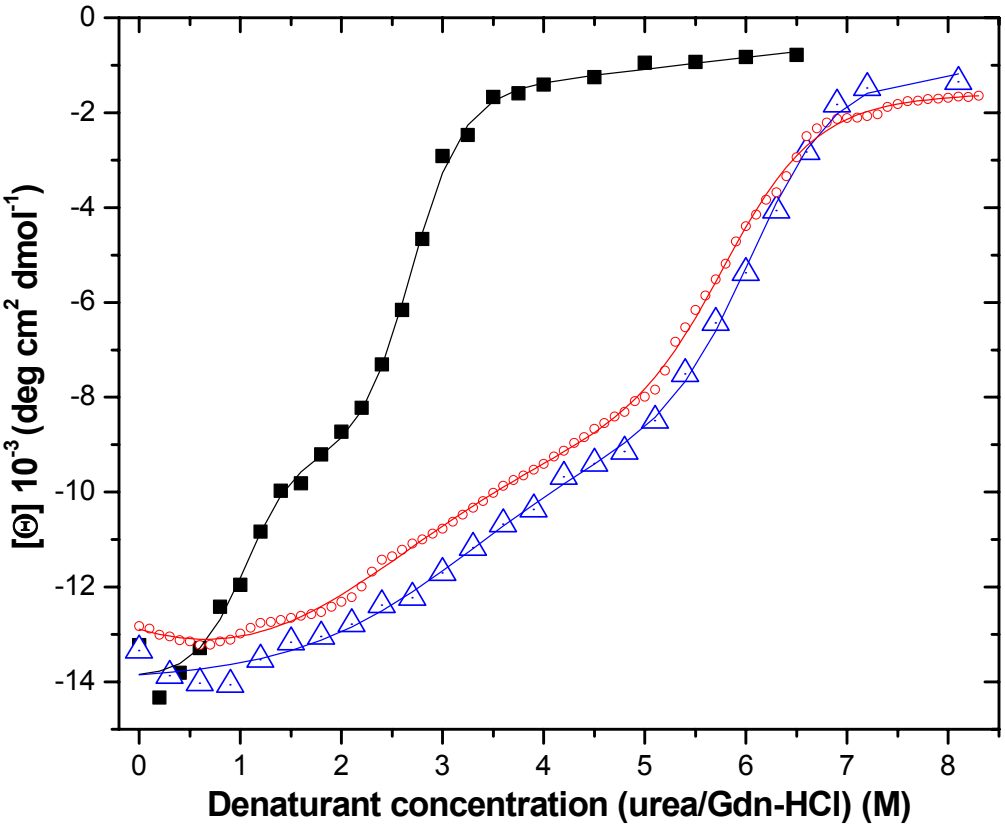

Figure 3.5: Denaturant-induced unfolding of β recombinase. Gdn-HCl induced unfolding of 3.65 E-6 M β monomers is represented by black squares. Urea induced unfolding for 3.65 E-6 M and 3.65 E-5 M β monomers is represented by red circles and blue triangles, respectively. The solid lines represent fit curves according to model 3.1. Buffer I (50 mM sodium phosphate, 1 M NaCl and 5% glycerol; pH 7.5) containing denaturant concentrations as indicated. CD ellipticity changes were measured at 222 nm and 20°C.

Table 3.1: Thermodynamic parameters for the fit of β recombinase equilibrium unfolding data to a three-state dimer denaturation model with a monomeric intermediate. The subscripts for *m* and ΔG refer to the *m* and ΔG values for the conversion of the native protein (N_2) to the intermediate, folded monomer (I) and the intermediate to the unfolded monomer (U) in accordance with model 3.1. All protein concentrations are in monomer equivalents, total concentration is $C=2[N_2] + [I] + [U]$

Denaturant	β conc. (M)	Transition I $N_2 \leftrightarrow I$			Transition II $I \leftrightarrow U$		
Urea	3.65 E-6	C_m	$\Delta G_{N\rightarrow I}$ [a]	$m_{N\rightarrow I}$ [b]	C_m	$\Delta G_{I\rightarrow U}$ [a]	$m_{I\rightarrow U}$ [b]
		3.5	4.33±0.067	1.37±0.19	5.9	6.42±0.55	1.1±0.1
	3.65 E-5	3.5	4.12±0.4	1.14±0.3	5.9	8.0±2.3	1.34±0.4
Gdn-HCl	3.65 E-6	1.0	4.15±1.4	3.14±2.6	2.5	6.13±0.5	2.3±0.18

[a] in kcal/mol
[b] in kcal/liter

ΔG_1 = 4.2 kcal/mol; $K_1 = 7.4 \times 10^{-4}$; ΔG_1 = 6.85 kcal/mol; $K_2 = 7.58 \times 10^{-6}$
$\Delta G_{tot} = \Delta G_1 + 2 \times \Delta G_2$
$\Delta G_{tot} = 4.2 + 2 \times 6.85 =$ **17.9 kcal/mol**

$K = K_1 \times K_2^2$
$K = 7.4E\text{-}4 \times (7.58\ E\text{-}6)^2$
$K = 4.25\ E\text{-}14$
$\ln K = \ln 4.25\ E\text{-}14 = -30.78$
$\Delta G = -RT \ln K = -0.583 \times -30.78 =$ **17.9 kcal/mol**

Global analysis was performed with the non-linear, least squares fitting program ORIGIN, ver 6.1. Errors quoted are the standard errors calculated by the fitting program.

3.1.5. Temperature-induced denaturation

3.1.5.1. Circular dichroism

Thermal melting of β recombinase at 1.8 μM β_2 was monitored by circular dichroism at 222 nm in the temperature range from 5°C to 90°C (Figure 3.6 and

3.7). CD spectra at selected temperatures are illustrated in Figure 3.6. In Figure 3.7, loss of negative ellipticity from -11 · 10^3 to -4.5 · 10^3 deg·cm^2·dmol^{-1} was observed. Three linear sections can be seen in the melting curve, first between 5 and 40°C, second from 40 to 70°C, and the third from 70 to 90°C. It is difficult to determine half transition temperatures from the CD melting curves.

Reversibility of unfolding was checked by slow cooling of sample back to 20 °C from 90 °C. ~70 % reversibility was observed (Figure 3.8).

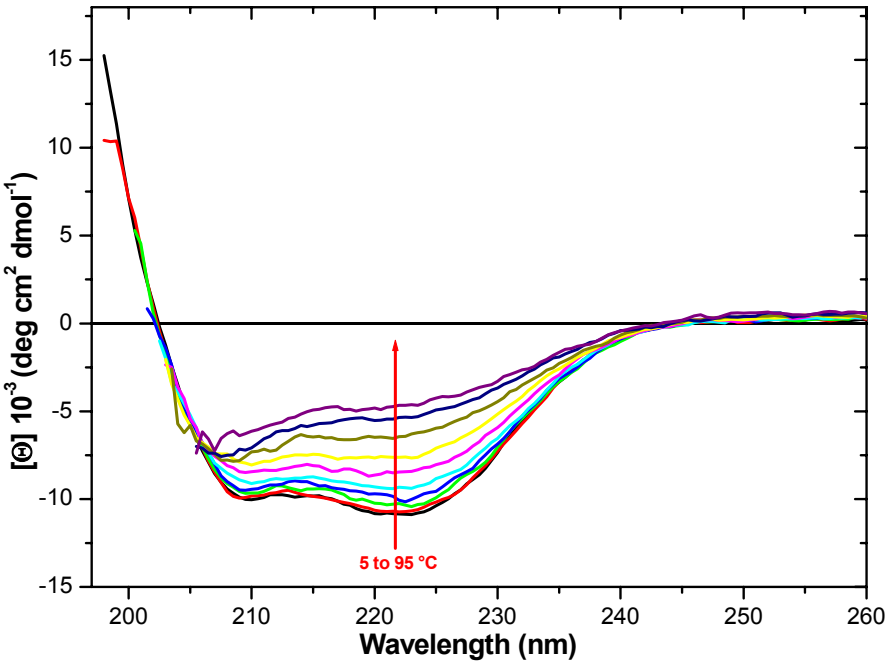

Figure 3.6: Thermal unfolding of β recombinase, spectra at selected temperatures. 1.8 μM β_2 was measured in buffer I (50 mM sodium phosphate, 1 M NaCl and 5% glycerol, pH 7.5).

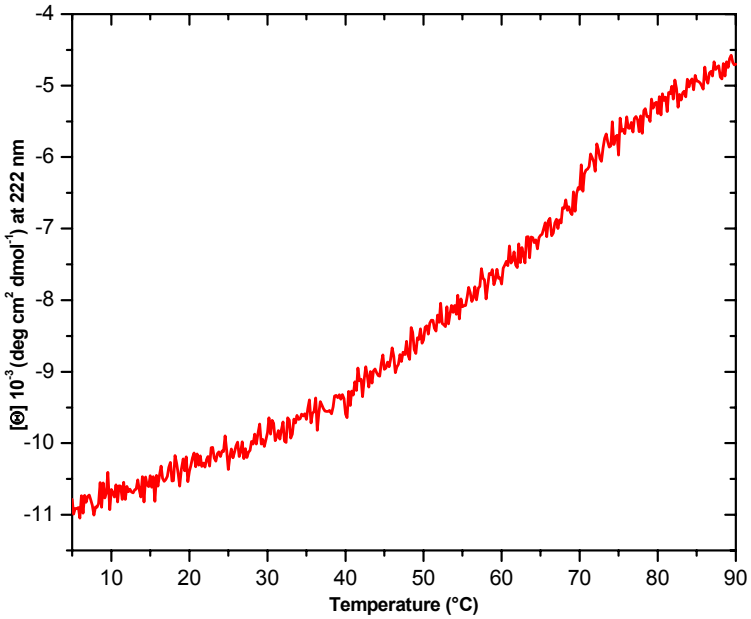

Figure 3.7: Thermal unfolding of β recombinase. CD ellipticity was measured at 222 nm with 1.8 μM β_2 in buffer I (50 mM sodium phosphate, 1 M NaCl and 5% glycerol, pH 7.5).

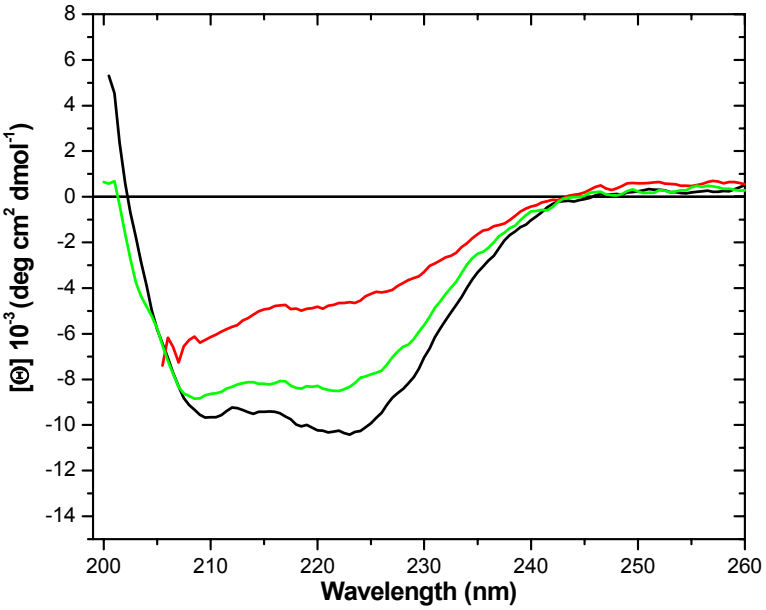

Figure 3.8: Thermal unfolding of β recombinase including renaturation spectra. Black, red and green represents spectra at 20, 90 and back to 20 °C, respectively.

3.1.5.2. Differential scanning calorimetry

The thermal unfolding of 18.5 µM and 4.2 µM β_2 has been examined by differential scanning calorimetry and were similar for both protein concentrations (Figure 3.9). The classical two-state model N ↔ U was applied for the deconvolution and provided a reasonable fit of the experimental curves (*177*). Transition temperatures T_m of 68.1°C and 67.4°C ± 0.2 with an unfolding enthalpy ΔH^{cal} of 114±1.2 kcal/mol and 105±5.9 kcal/mol has been calculated for 18.5 µM and 4.2 µM β_2, respectively, the ratio of $\Delta H^{cal}/\Delta H^{vH}$ was close to unity (Table 3.2). A second run after cooling of the sample from 90 °C to 20 °C indicated about ~85% reversibility of unfolding.

This follows from the fact that thermal melting monitored by differential scanning calorimetry fits were obtained for a two state unfolding of native dimers N_2 into unfolded dimers U_2 according to $N_2 \leftrightarrow U_2$.

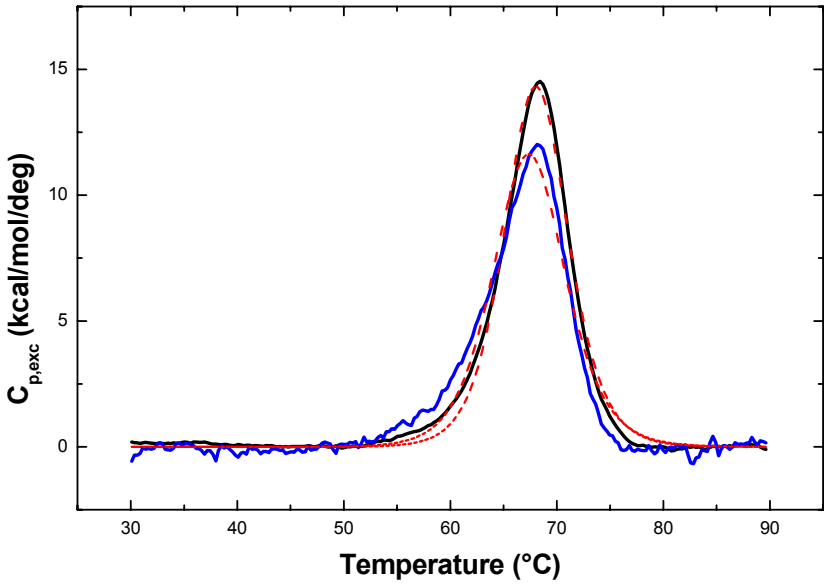

Figure 3.9: Fitted DSC curves of β recombinase. Best fit of the experimental DSC tracing obtained for β recombinase in buffer I (50 mM sodium phosphate buffer, 1 M NaCl and 5% glycerol, pH 7.5) using β_2 concentrations of 4.2 µM (blue) and 18.5 µM (black). The corresponding red lines are fits performed according to a “two-state" model.

Table 3.2: Thermodynamic parameters for the β recombinase obtained by the model analysis of DSC thermograms. Model independent calorimetric enthalpy (ΔH^{cal}) values were determined by integration of the corresponding DSC thermograms.

β_2 Concentration (M)	Transition temperature T_m (°C)	Calorimetric enthalpy (ΔH^{cal}) (kcal/mol)	Van't Hoff enthalpy (ΔH^{vH}) (kcal/mol)
18.5 μM	68.08 ±0.04	114 ±1.2	116 ±1.5
4.2 μM	67.41 ±0.23	105 ±5.9	102 ±7.18

3.2. Discussion

The CD spectrum of β recombinase indicated a high α-helical content in agreement with the secondary structure predictions and with the structure of the related γδ resolvase bound to site I (Figure 3.1). Formation of dimers and high α-helical content are common features of many DNA-binding proteins (*181-183*). Gel filtration chromatography and sedimentation equilibrium analytical ultracentrifugation experiments were used to determine the oligomeric state of the β recombinase. Gel filtration chromatography showed a retention volume characterized by a single sharp and symmetrical peak corresponding to molecular mass of 52 ± 2 kDa in buffer containing 1 M NaCl (Figure 3.3). Unlike wild type β recombinase that is a dimer in solution at high ionic strength (this report), resolvase or DNA invertase proteins are mainly monomers in solution (*32, 45, 49, 50*). Upon binding to DNA a considerable conformational change in the subunit structure of the dimer will be a prerequisite for catalysis (*46*). We cannot rule out that even β recombinase, in the absence of DNA, forms tetramers in solution. It is likely that in the hyperactive mutant resolvase or DNA invertases, with certain mutation(s) within or near the dimerization E helix (*32-34, 46, 51, 53, 184*) and in the wild type β_2 recombinase, the tetramerization potential is stabilized *with the consequence that* the active-site serine residues are positioned suitably to attack the DNA backbone (*26*).

The dimeric state prior DNA binding is of high relevance if manipulations of eukaryotic genomes are to be considered, because the affinity of dimeric β recombinase to non-specific binding sites should be lower that the affinity of a monomeric serine recombinase to non-specific DNA binding sites on the eukaryotic genome. This is consistent with the observation that the affinity of monomeric Tn*3* resolvase to cognate site increases the affinity to non-cognate site 10-fold (*50*).

The purified β recombinase visibly aggregated and precipitated in low-ionic-strength buffers (< 300 mM NaCl) in the absence of DNA at near neutral pH, a behavior similar to that of other members of serine recombinase family (*49, 159, 185*). This behavior rendered difficult any further analysis at low salt concentration; therefore we used a constant concentration of 1 M NaCl in all of our experimental buffers, where β recombinase has well-defined dimer state. Moreover, the sedimentation equilibrium experiments showed a single-exponential distribution of β recombinase in the cell. Fitting independent data sets at different protein concentrations and rotor speeds to a single species model gave the molecular mass of dimer in-between experimental temperatures of 4 and 25 °C and down to sub-micromolar protein concentrations (Figure 3.3 and 3.4). The concentration of dimers and monomers are related through the dissociation constant K_d = [Monomer]^2/[Dimer]. At 3 μM β_2, the protein is still a dimer. Figure 3.4 indicating that monomer association was relatively strong under the conditions used. This is in contrast with the K_d = 50 μM or higher concentration for monomer-dimer dissociation constant of the Tn*3* or γδ resolvases (*49, 50*).

The overall unfolding pathway for dimeric proteins begins with the folded dimer and usually ends with unfolded monomers. Folded monomers may occur as intermediates of the unfolding. Numerous examples exist for both compact monomeric and dimeric intermediates that are significantly populated during the equilibrium denaturation of a folded dimer (*186-192*).

Monomeric or dimeric intermediates could be formed during a three state unfolding of β_2 by urea and Gdn-HCl as described by model 3.1 and model 3.2.

$N_2 \xleftrightarrow{K_{1A}} 2I \xleftrightarrow{K_{2A}} 2\,U$ Model 3.1

OR

$N_2 \xleftrightarrow{K_{1B}} I_2 \xleftrightarrow{K_{2B}} 2\ U$ Model 3.2

N_2 is native folded dimer, I is folded monomeric intermediate, I_2 is folded dimeric intermediate, and U is unfolded monomer. Urea and Gdn-HCl unfolding curves of β recombinase are characterized by inflexion points at about 5 M urea and 2.2 M Gdn-HCl (Figure 3.5). Dissociation of β_2 into β monomers might be a reasonable possibility to explain the slow and linear, non-cooperative increase of the negative molar ellipticity between 2 M and 5 M urea. Between 5 and 6.5 M urea the slope of the unfolding curve was steeper and suggested the formation of unfolded monomers.

Dissociation of dimers into monomers is a bimolecular reaction and the equilibrium populations of dimers and monomers should be protein dependent. Considering the concentration dependence of the unfolding of dimeric protein, it is obvious that the concentration of any monomeric or dimeric intermediate depends on the values of K_{1A}, K_{2A}, and K_{1B}, K_{2B}, and the total concentration of protein. The equilibrium dissociation constants are $K_{1A} = [I]^2 / [N_2]$ and $K_{2A} = [U] / [I]$ for three-state model 3.1with monomeric intermediate and $K_{1B} = [I_2] / [N_2]$ and $K_{2B} = [U]^2 / [I_2]$ for model 3.2 with dimeric intermediate.

If a monomeric intermediate [I] is involved, the first step of the unfolding reaction is bimolecular and depends on the protein concentration. [I] increases with the square root of $[N_2]$. It follows that the equilibrium unfolding of the first transition in a dimeric system with a monomeric intermediate is expected to shift to higher temperature or denaturant concentration with increasing protein concentration, and the slope of the unfolding curve will increase.

If according to model 3.2 a dimeric intermediate $[I_2]$ is involved, the ratio of $[I_2]$ to $[N_2]$ remains the same for all protein concentrations, as the first step of unfolding is monomolecular and not protein concentration dependent. However,

$[I_2]$ increases with the total protein concentration, therefore in second step which is bimolecular, [U] increases proportional to the square root of $[I_2]$. Overall, this will lead to an increase in the fraction of $[I_2]$. Therefore, for model 3.2 with dimeric intermediate, the slope of the transition will decrease with increasing protein concentration, due to an increased population of the intermediate state. Results show that this is not the case for β recombinase, making a dimeric intermediate unlikely (Figure 3.5). For β_2, rather a monomeric intermediate but not a dimeric intermediate can be deduced from the unfolding curves (Figure 3.5, compare circles and triangles). However, in our urea unfolding measurements at β_2 concentrations of 1.83 μM and 18.3 μM, only small differences were observed that did not provide convincing evidence fot the expected stability increase at higher protein concentration.

Analytical ultracentrifugation provides an independent, strong argument for the identification of the intermediate. To determine the molecular masses at 5 M and 8 M urea sedimentation equilibrium analysis indicated monomers. This finding is consistent with the presence of folded monomers at 5 M urea and unfolded monomers at 8 M urea which cannot be discriminated by analytical ultracentrifugation (Figure 3.4).

Interestingly, differential calorimetry of β recombinase did not reveal the formation of intermediates or differential melting of domains. A good fit of the experimental melting curves was obtained with the classical two state model, N ↔ U. This is surprising in view of the expectation of two domains per β recombinase monomer and, more important, the presence of β_2 dimers under the experimental conditions. Thus, the result suggested an unfolding model where folded dimers thermally unfold into unfolded dimers according to

$$N_2 \leftrightarrow U_2 \qquad \text{(Model 3.3)}$$

Experimental DSC curves were similar for 4.2 μM and 18.5 μM β_2 (Figure 3.9). The same values of ΔH^{cal} were obtained for 4.2 μM and 18.5 μM β_2; and the ratio $\kappa=\Delta H^{cal}/\Delta H^{vH}$ was close to unity (Table 3.2). Such a model would be completely different from that suggested by the denaturant induced unfolding experiments ($N_2 \xleftrightarrow{K_{1A}} 2I \xleftrightarrow{K_{2A}} 2\ U$). The formation of denatured dimers was recently described upon thermal denaturation several systems (*193-195*). A sequence depending oligomerization has been observed in the Arc repressor system (*194*). For the thermal unfolding of the ParD repressor similar observations were made, but interpreted as a single two-state transition of two coupled monomers (*195*) Alternatively, ParD unfolding might be considered as a transition of folded to unfolded dimers, in agreement with observations for Arc or Omega transcriptional repressors (*193*) and the data described here. Thermally induced formation might be result of regions with “sticky” sequences. Possibly these regions are already in contact in the folded state and interact by forces that increase their strength with increasing temperatures, thus fixing the dimeric state. Otherwise, “sticky” regions might become exposed at high temperatures and form unfolded dimers by new interactions.